Diabetologia (2011) 54:2595–2605
DOI 10.1007/s00125-011-2255-9

ARTICLE

The Krüppel-like zinc finger protein GLIS3 transactivates neurogenin 3 for proper fetal pancreatic islet differentiation in mice

Y. Yang · B. H-J. Chang · V. Yechoor · W. Chen · L. Li · M.-J. Tsai · L. Chan

Received: 7 May 2011 / Accepted: 14 June 2011 / Published online: 23 July 2011

Abstract
Aims/hypothesis Mutations in *GLIS3*, which encodes a Krüppel-like zinc finger transcription factor, were found to underlie sporadic neonatal diabetes. Inactivation of *Glis3* by gene targeting in mice was previously shown to lead to neonatal diabetes, but the underlying mechanism remains largely unknown. We aimed to elucidate the mechanism of action of GLIS family zinc finger 3 (GLIS3) in *Glis3*$^{-/-}$ mice and to further decipher its action in in-vitro systems.
Methods We created *Glis3*$^{-/-}$ mice and monitored the morphological and biochemical phenotype of their pancreatic islets at different stages of embryonic development. We combined these observations with experiments on *Glis3* expressed in cultured cells, as well as in in vitro systems in the presence of other reconstituted components.
Results In vivo and in vitro analyses placed *Glis3* upstream of *Neurog3*, the endocrine pancreas lineage-defining transcription factor. We found that GLIS3 binds to specific GLIS3-response elements in the *Neurog3* promoter, activating *Neurog3* gene transcription both directly, and synergistically with hepatic nuclear factor 6 and forkhead box A2.
Conclusions/interpretation These results indicate that GLIS3 controls fetal islet differentiation via direct transactivation of *Neurog3*, a perturbation that causes neonatal diabetes in mice.

Keywords GLIS3 · Neonatal diabetes · Neurog3 · Pancreatic islet differentiation

Abbreviations

BAC	Bacterial artificial chromosome
ChIP	Chromatin immunoprecipitation
E	Embryonic day
EMSA	Electrophoretic mobility shift assay
FOXA2	Forkhead box A2
GLIS3	GLIS family zinc finger 3
GLIS3RE	GLIS3 response element
HNF1B	HNF1 homeobox B
HNF6	Hepatic nuclear factor 6
MAFA	v-Maf musculoaponeurotic fibrosarcoma oncogene family, protein A (avian)
NDH	Neonatal diabetes and congenital hypothyroidism
NEUROG3	Neurogenin 3
NKX6-1	NK6 homeobox 1
NOTCH	Notch gene homologue
P	Postnatal day
PDCs	Pancreatic ductal cells
PDX1	Pancreatic and duodenal homeobox 1
SOX9	SRY-box containing gene 9
YFP	Yellow fluorescent protein

Electronic supplementary material The online version of this article (doi:10.1007/s00125-011-2255-9) contains peer-reviewed but unedited supplementary material, which is available to authorised users.

Y. Yang · V. Yechoor · W. Chen · L. Chan (✉)
Diabetes and Endocrinology Research Center,
Division of Diabetes, Endocrinology and Metabolism,
Department of Medicine, Baylor College of Medicine,
One Baylor Plaza,
Houston, TX 77030, USA
e-mail: lchan@bcm.edu

B. H.-J. Chang · L. Li · M.-J. Tsai · L. Chan
Department of Molecular and Cellular Biology,
Baylor College of Medicine,
Houston, TX, USA

L. Chan
Department of Internal Medicine, St Luke's Episcopal Hospital,
Houston, TX, USA

Introduction

Monogenic neonatal diabetes is characterised by beta cell dysfunction within 6 months of age, rendering affected individuals transiently or permanently diabetic, and requiring insulin or other treatments for survival [1, 2]. Permanent neonatal diabetes usually results from mutations of genes encoding transcription factors or other proteins that regulate beta cell development or function [3]. A novel autosomal recessive disorder featuring permanent neonatal diabetes was described recently by Taha et al. [4], and linkage analysis of affected families identified *GLIS3*, which encodes a member of the Krüppel-like family of transcription factors [5], as the mutant gene underlying this syndrome [6]. The demonstration of mutant *GLIS3* in families with neonatal diabetes is intriguing; however, the underlying pathogenetic mechanism linking the *GLIS3* locus to abnormal glucose homeostasis in neonates is unknown.

GLIS3 is expressed in human and mouse pancreas from early developmental stages through to adulthood, with higher expression in beta cells than in other islet or exocrine cells [6]. We have previously shown that *Glis3* directly regulates insulin gene expression; we also identified a GLIS family zinc finger 3 (GLIS3) response element (GLIS3RE) in the insulin promoter [7]. The recent description of neonatal diabetes in *Glis3*-deficient mice by two different groups [8, 9] supports a pivotal role of GLIS3 in beta cell function during fetal development. Watanabe et al. first reported that inactivation of *Glis3* produced neonatal diabetes in mice [8]. A subsequent study by Kang et al. [9] found a dramatic loss of beta and delta cells, with a more modest loss of alpha, pancreatic polypeptide and epsilon cells in the *Glis3* mutant mouse pancreas. The same team also showed that the expression of several genes encoding transcription factors involved in the regulation of endocrine differentiation, including *Pdx1*, *Neurog3*, *Nkx6-1*, *Pax4*, *Pax6*, *Isl1*, *Neurod1* and *Mafa*, was significantly decreased in the pancreas of *Glis3* mutant mouse. However, neither of the two studies [8, 9] reported the precise function of *Glis3*, and particularly whether and how GLIS3 regulates *Neurog3* expression in pancreatic islet development.

To gain insight into the physiological and pathophysiological roles of GLIS3, we created $Glis3^{-/-}$ mice, which die with severe hyperglycaemia and ketoacidosis within 4 to 6 days of birth. The pancreatic islets of these mice were much smaller and poorly organised as compared with controls. Neurogenin 3 (NEUROG3), a basic helix–loop–helix pancreatic islet lineage-defining transcription factor, is essential to pancreatic islet formation [10–13]. Here we show that GLIS3 is involved in the differentiation of endocrine progenitor cells through direct and indirect transcriptional control of *Neurog3* expression. The combination of in vivo and in vitro experiments identified GLIS3 as a key regulator of islet morphogenesis during embryonic development and provided the mechanistic basis for a crucial role of GLIS3 in fetal islet differentiation and neonatal diabetes.

Methods

Glis3 gene targeting and generation of global Glis3 targeted mice We purchased a bacterial artificial chromosome (BAC) clone (RP23-358 M17) containing the mouse *Glis3* gene from Invitrogen (Carlsbad, CA, USA). Two DNA fragments, 2.5 and 7.2 kb, were subcloned from this BAC by recombineering [14] and used for homologous recombination. A 1.4 kb DNA fragment containing the targeted exon 4 with its immediate 5′ and 3′ introns (partial) was amplified by PCR and inserted in between two loxP sites of the NeoFrtLoxP vector. Two TK cassettes were inserted into the 5′-end of the targeting vector.

We electrophorated R1 mouse embryonic stem cells [15] with a linearised targeting construct, and selected embryonic stem cells with G418 (Invitrogen) and ganciclovir. Blastocyst injection and germline transmission were done by standard techniques.

To generate global *Glis3*-deficient mice, we bred $Glis3^{fl/fl}$ mice with protamine-Cre transgenic mice ($PrmCre^{+/0}$), which express Cre in sperm [16]. We then bred the $Glis3^{fl/+}/PrmCre^{+/0}$ males with C57BL/6 J females to generate $Glis3^{+/-}/PrmCre^{0/0}$ mice, which are essentially heterozygous mutant mice ($Glis3^{+/-}$). Cross-breeding of these mice produced homozygous deletion of *Glis3* ($Glis3^{-/-}$). Mice used in this study were maintained in a barrier facility. All mouse protocols were approved by the Institutional Animal Care and Use Committee (IACUC) at Baylor College of Medicine.

Glucose, insulin and ketone body measurement Glucose level was measured using a glucometer (One Touch; Lifescan, Milpitas, CA, USA). We measured plasma insulin using a mouse ELISA kit (Mercodia, Winston Salem NC; Millipore, Billerica, MA, USA) and β-hydroxybutyrate (ketone body) with a kit (Cayman Chemical, Ann Arbor, MI, USA). To measure pancreatic insulin content, we homogenised neonatal whole pancreas at postnatal day (P) 0 in 0.2 mmol/l HCl with 70% (vol./vol.) ethanol. After neutralisation with 1 mol/l Tris HCl (pH 7.5), insulin was measured using a mouse ELISA kit (Mercodia) with the appropriate dilution.

Immunofluorescence staining We performed immunostaining on paraffin-embedded, 5- to 7-μm sections of whole embryos collected at embryonic day (E)12.5 and E15.5, or of dissected pancreas, which were fixed in freshly made 4%

(wt/vol.) paraformaldehyde in PBS. Primary antibodies were: guinea pig anti-insulin (Abcam, Cambridge, MA, USA); rabbit anti-glucagon, rabbit anti-pancreatic polypeptide and rabbit anti-somatostatin (Dako, Carpinteria, CA, USA); goat anti-ghrelin (Santa Cruz Biotechnology, Santa Cruz, CA, USA); goat anti-pancreatic and duodenal homeobox 1 (PDX1) antibody (gift of C. Wright, Vanderbilt University, Nashville, TN, USA); mouse anti-NEUROG3 and anti-NK6 homeobox 1 (NKX6-1) (Developmental Studies Hybridoma Bank, University of Iowa, Iowa City, IA, USA); anti-v-maf musculoaponeurotic fibrosarcoma oncogene family, protein A (avian) (MAFA) antibody (Bethyl Laboratories, Montgomery, TX, USA); and anti-cleaved caspase-3 antibody (Cell Signaling, Danvers, MA, USA). The primary antibodies were detected with secondary antibodies conjugated to FITC, Cy5 or rhodamine (Invitrogen). We used an Axiovert (Carl Zeiss AG, Jena, Germany) microscope with Axiovision imaging software to capture fluorescent images and did post-acquisition image processing with Adobe Photoshop (San Jose, CA, USA).

Islet area and positive cell quantification We estimated islet area and endocrine-positive cell area using ImageJ 1.4 (NIH, Bethesda, MD, USA) on four haematoxylin and eosin stained or fluorescent sections (approximately every tenth section) that had been processed from four independent pancreases. For quantification of NEUROG3-positive cells, we counted the absolute number of positive cells on five (*Glis3*$^{+/+}$) and ten (*Glis3*$^{-/-}$) embryonic sections from at least five different mice for each genotype.

In situ hybridisation We performed non-radioactive in situ hybridisation with digoxigenin-UTP (Roche Diagnostics, Indianapolis, IN, USA)-labelled antisense RNA probes using a 645-bp full length mouse *Neurog3* cDNA clone; this was done in collaboration with the Gene Expression Core at Baylor College of Medicine.

Cell culture studies We obtained pancreatic ductal cells (PDCs) from A. K. Rustgi (University of Pennsylvania, School of Medicine, Philadelphia, PA, USA) and maintained them as described by Schreiber et al. [17]. We transduced PDCs with pMSCV (Clontech, Mountain View, CA, USA)-*Glis3* retroviral construct and maintained rat 832/13 insulinoma cells (gift of C. Newgard, Duke University, Durham, NC, USA) as described previously [7]. We cultured HepG2 cells in RPMI 1640 with 10% (vol./vol.) FBS. We used Lipofectamine 2000 (Invitrogen) for transfection according to the manufacturer's instructions.

Luciferase reporter constructs and assays Using RT-PCR, we amplified the coding sequences of mouse *Glis3*, *Pdx1*, *Hnf6* (also known as *Onecut1*), *Sox9*, *Foxa2* and *Hnf1b*, and cloned them into a *c-myc*-tagged pBOS-MCS vector [18]. A mutant *Glis3* cDNA that corresponds to the sequence in a family with neonatal diabetes and congenital hypothyroidism (NDH) syndrome was constructed (*Glis3*-NDH1) as described previously [7]. A 5.8 kb mouse *Neurog3* promoter fragment (SacI/KpnI), modified from *Neurog3-CreER* plasmid (Addgene, Cambridge, MA, USA), was cloned into a pGluc-basic (New England Biolabs, Ipswich, MA, USA) vector to generate a *Neurog3*-Gluc reporter construct. Wild-type and mutant (GLIS3RE)5-Gluc constructs were made as described previously [7]. All expression constructs were confirmed by DNA sequencing. At 48 h after transfection, gaussia luciferase assays were performed as described previously [7] and results normalised to the activity of β-galactosidase reporter (Sigma, Ronkonkoma, NY, USA).

RNA isolation and quantitative PCR A kit (Mini RNA Isolation I; Zymo Research, Irvine, CA, USA) was used to extract RNA from the E13.5 pancreases. Reverse transcription and quantitative PCR were performed as described previously [7]. The housekeeping gene cyclophilin A was used as an internal control. Primer sequences are shown in electronic supplementary material [ESM] Table 1.

Co-immunoprecipitation assays We performed co-immunoprecipitation assays using a nuclear complex co-immunoprecipitation kit (Active Motif, Carlsbad, CA, USA) as described previously [7].

Chromatin immunoprecipitation We performed chromatin immunoprecipitation (ChIP) assays in PDCs infected with the pMSCV-*c-myc*-yellow fluorescent protein (YFP) or -GLIS3 retroviral constructs as described previously [7]. For E13.5 pancreas ChIP, 65 to 100 pancreases were isolated from C57BL/6 E13.5 embryos, snap-frozen in liquid nitrogen and stored at −80°C until use. Frozen pancreases were pooled and thawed on ice, and cross-linked immediately in 1.5% (wt/vol.) formaldehyde at room temperature for 15 min, followed by ChIP assays.

Electrophoretic mobility shift assay Electrophoretic mobility shift assays (EMSA) were conducted using a biotin-labelled double-stranded oligonucleotide probe containing the recognition sequence for *Glis3* (ESM Table 1) as described previously [7].

GLIS3 antibody Rabbit anti-mouse GLIS3 peptide (LSAVDRCPSQLSSVYTEG) antibody was generated by Thermo Fisher Scientific (Waltham, MA, USA).

Statistical analysis The standard Student's two-tailed *t* test was used for comparisons. Results are presented as the mean±SD unless otherwise specified.

Results

Post-natal growth retardation and severe neonatal diabetes in Glis3$^{-/-}$ mice The strategy for creation of *Glis3*$^{-/-}$ mice is shown online in ESM Fig. 1a. We targeted exon 4 of mouse *Glis3* gene, resulting in a premature termination codon in exon 6 (exon 5 162 bp). *Glis3* mRNA was undetectable by quantitative RT-PCR in RNA isolated from the pancreas of *Glis3*$^{-/-}$ mice (ESM Fig. 1b). *Glis3*$^{-/-}$ mice had no intrauterine growth retardation (ESM Fig. 1c), fed normally and were indistinguishable from their wild-type littermates at birth. However, they showed growth arrest and became smaller starting from P1 as compared with control mice. By P4, they were dehydrated and much smaller. All *Glis3*$^{-/-}$ mice died between P4 and P6 (ESM Fig. 2a, b).

Although *Glis3*$^{-/-}$ mice appeared normal at birth, their blood glucose level was mildly but significantly higher than that of *Glis3*$^{+/-}$ or *Glis3*$^{+/+}$ littermates on P0 (day of birth) (ESM Fig. 2c). By P4, *Glis3*$^{-/-}$ mice exhibited marked hyperglycaemia (>33.3 mmol/l) while their littermate controls remained euglycaemic (ESM Fig. 2c). Hyperglycaemia in *Glis3*$^{-/-}$ mice was associated with severe hypoinsulinaemia, with plasma insulin (ESM Fig. 2d) and pancreatic insulin content (ESM Fig. 2e) markedly decreased as compared with control littermates. *Glis3*$^{-/-}$ mice also displayed severe ketonaemia on P4 (ESM Fig. 2f). Our data corroborate and extend those published in two previous studies on *Glis3*$^{-/-}$ mice [8, 9].

Defective islet cell differentiation in Glis3$^{-/-}$ mice To investigate the defect associated with insulin deficiency in *Glis3*$^{-/-}$ mice, we performed histological and immunofluorescence analyses on mouse embryos. At E12.5, immunoreactive glucagon and insulin-positive cells were detected in the pancreas of *Glis3*$^{+/+}$ but not in that of *Glis3*$^{-/-}$ mice (data not shown). By E15.5, although glucagon- and insulin-positive cells were detectable in *Glis3*$^{+/+}$ and *Glis3*$^{-/-}$ mice, both types of cells were significantly decreased in the latter (ESM Fig. 3a–d). At E17.5, the abundance of immunoreactive insulin, glucagon, somatostatin and ghrelin was markedly decreased in the islets of *Glis3*$^{-/-}$ mice (ESM Fig. 3e–j) as compared with controls.

The total pancreas:body weight ratio on P0 was normal in *Glis3*$^{-/-}$ mice (ESM Table 2). However, islets were much smaller and were poorly organised morphologically in neonatal *Glis3*$^{-/-}$ mice (Fig. 1a, b). The total islet area of *Glis3*$^{-/-}$ neonatal mice, as estimated from tissue sections, was only 15% of that in *Glis3*$^{+/+}$ littermates (Fig. 1c). *Glis3*$^{-/-}$ mice showed markedly reduced numbers of alpha, beta, delta, pancreatic polypeptide and epsilon cells, as indicated by immunostaining of glucagon, insulin, somatostatin, pancreatic polypeptide and ghrelin, respectively. Quantitative analyses of immunofluorescence-positive cell areas showed that the relative reductions were 71.3%, 83.1%, 87.6%, 79.8% and 86.1% for the alpha, beta, delta, pancreatic polypeptide and epsilon cells, respectively (Fig. 1d–o).

As the numbers of all types of endocrine cells were uniformly reduced in the neonatal *Glis3*$^{-/-}$ mice, we examined apoptosis by cleaved caspase-3 immunostaining and found that the number of apoptotic islet cells was similar in *Glis3*$^{-/-}$ mice and *Glis3*$^{+/+}$ littermates (ESM Fig. 4a, b). Furthermore, the exocrine pancreas was normal histologically and levels of the exocrine enzyme, amylase, remained unchanged in the pancreas of *Glis3*$^{-/-}$ mice (ESM Fig. 4c, d).

Absence of Glis3 leads to reduced abundance of key pancreatic endocrine differentiation transcription factors To further characterise the perturbed endocrine pancreas development in *Glis3*$^{-/-}$ embryos, we used immunofluorescence to analyse the abundance of key pancreatic transcription factors at various stages. PDX1 and NKX6-1 are two transcription factors whose production marks endodermal epithelium cells that have been specified to a pancreatic fate [10, 19–21]. At E12.5, the abundance of PDX1 and NKX6-1 was normal in the *Glis3*$^{-/-}$ pancreas (ESM Fig. 5a–d), suggesting that early pancreatic epithelium specification was unperturbed in the absence of *Glis3*. However, by E15.5, the number of positive cells for PDX1, NKX6-1 and NEUROG3 was markedly reduced in *Glis3*$^{-/-}$ mice compared with *Glis3*$^{+/+}$ littermates (ESM Fig. 5e–h). At E17.5 and P0, numbers of positive cells for all four key pancreatic islet transcription factors, i.e. PDX1, NKX6-1, NEUROG3 and MAFA, were markedly decreased in the pancreas of *Glis3*$^{-/-}$ mice (ESM Fig. 5i–t).

Expression of the proendocrine gene Neurog3 is markedly reduced in Glis3$^{-/-}$ embryos Expression of *Neurog3* is crucial to pancreatic endocrine cell fate determination [10–13, 22]. Because all endocrine cell markers were reduced in the *Glis3*$^{-/-}$ pancreas, we performed quantitative RT-PCR to quantify *Neurog3* mRNA expression and found that it was significantly decreased in *Glis3*$^{-/-}$ pancreas at E13.5 compared with controls (Fig. 2a). In addition, quantitative RT-PCR showed that mRNA levels of *Neurod1* and *Isl1*, two downstream targets of *Neurog3* [23–25], were also significantly decreased in *Glis3*$^{-/-}$ pancreas at E13.5 compared with controls (Fig. 2a). Furthermore, in situ hybridisation showed that the number of cells positive for *Neurog3* mRNA was greatly diminished in *Glis3*$^{-/-}$ embryos at E12.5 and that in the few residual *Neurog3*-positive cells, the hybridisation signal was much weaker in *Glis3*$^{-/-}$ than in *Glis3*$^{+/+}$ embryos (Fig. 2b).

In agreement with the reduced *Neurog3* mRNA expression, NEUROG3-positive cells were also markedly decreased at the protein level as detected by immunofluorescence in

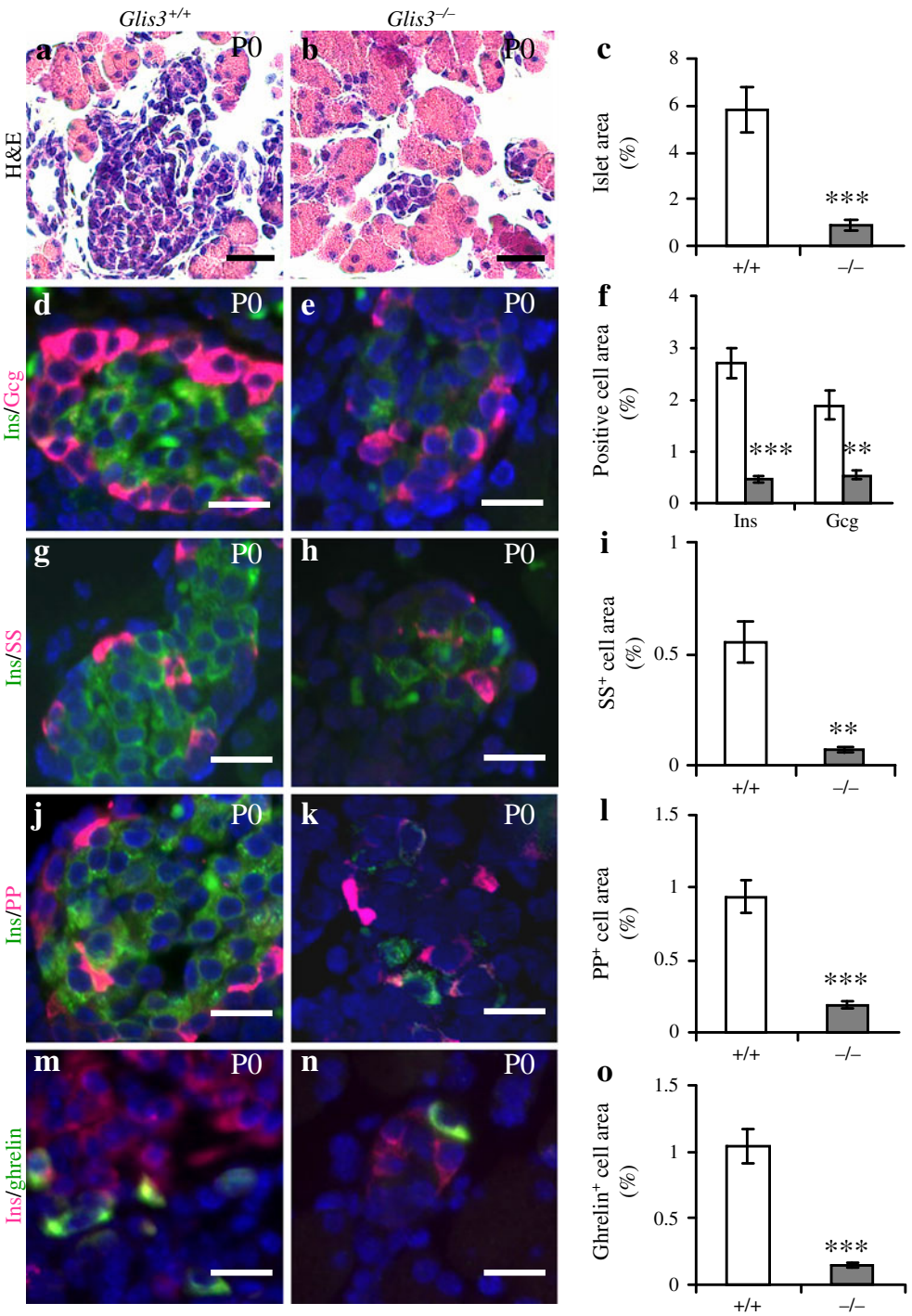

Fig. 1 Defective endocrine cell differentiation in *Glis3*$^{-/-}$ mice at P0. **a** Histology of pancreas by haematoxylin and eosin (H&E) staining in *Glis3*$^{+/+}$ and (**b**) *Glis3*$^{-/-}$ mice, with (**c**) islet area quantification. **d, e** Immunostaining and (**f**) quantification of cell areas positive for insulin (Ins, green) and glucagon (Gcg, red). **g, h** Immunostaining and (**i**) quantification of cell areas positive for insulin (green) and somatostain (SS, red), for (**j–l**) insulin (green) and pancreatic polypeptide (PP, red), and for (**m–o**) insulin (red) and ghrelin (green) in the pancreas of mice as labelled. **$p<0.01$, ***$p<0.001$ vs *Glis3*$^{+/+}$. Scale bars 20 μm

E12.5 *Glis3*$^{-/-}$ embryos (Fig. 2c). Quantification indicated that the number of the NEUROG3-positive cells was decreased by >95% (Fig. 2d).

To corroborate the loss-of-function findings in *Glis3*$^{-/-}$ mice and to determine whether expression of *Neurog3* is regulated by GLIS3, we performed a gain-of-function experiment by overexpressing *c-myc*-tagged *Glis3* in mouse PDCs, a well established cell type frequently used to study *Neurog3* expression and regulation [26–28]. Compared with cells transduced with the *c-myc*-YFP, overexpression of *c-myc-Glis3* was sufficient to stimulate endogenous *Neurog3* mRNA expression in PDCs (Fig. 2e, f), suggesting that *Neurog3* is a downstream target of *Glis3*.

Neurog3 gene expression is known to be upregulated by several transcription factors such as PDX1 [28–30], hepatic nuclear factor 6 (HNF6) [31], SRY-box containing gene 9 (SOX9) [32], forkhead box A2 (FOXA2) [33] and HNF1 homeobox B (HNF1B) [33, 34]. It is negatively regulated

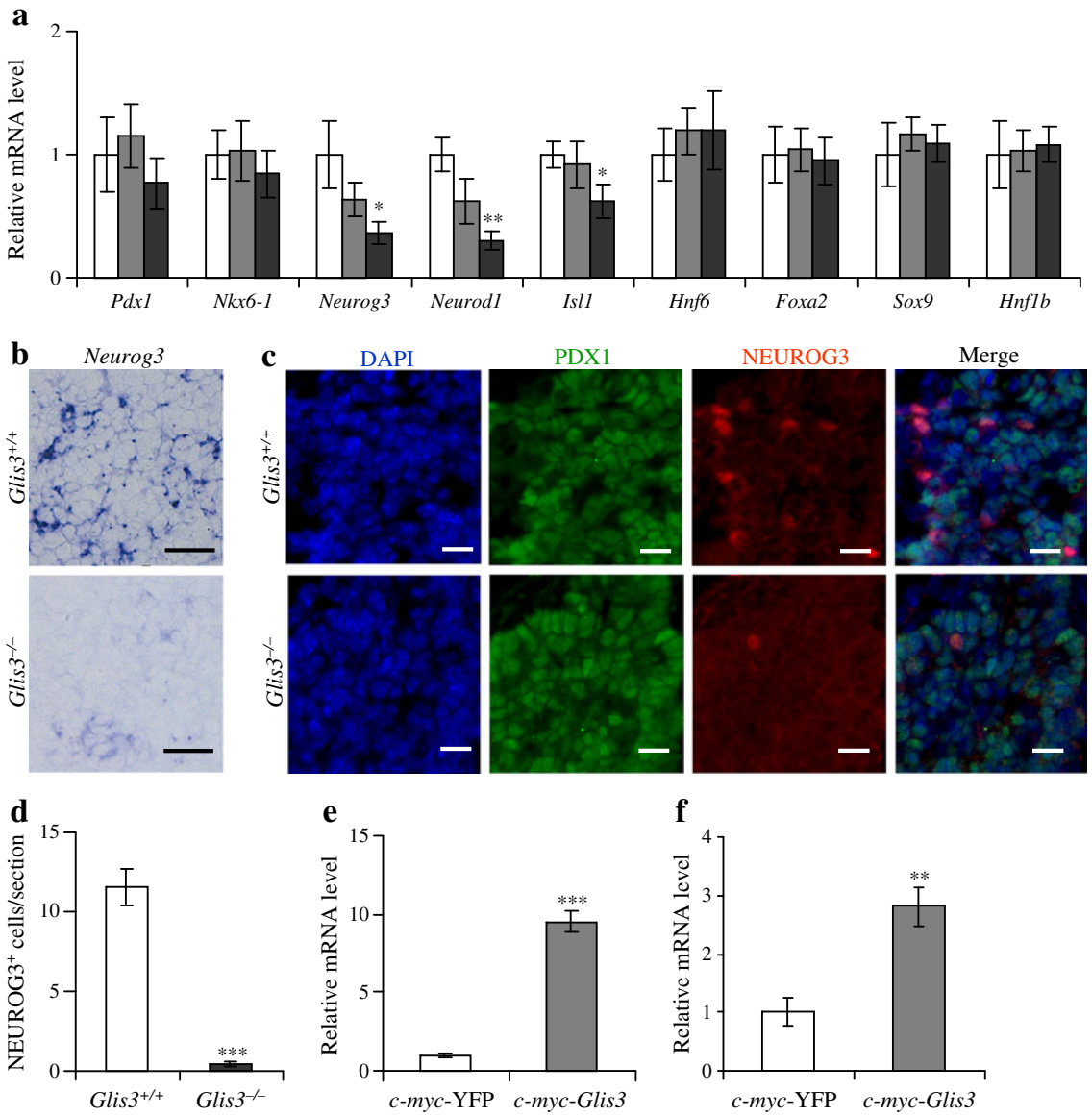

Fig. 2 GLIS3 regulates *Neurog3* expression in vivo and in vitro. **a** The mRNA expression of *Pdx1*, *Nkx6-1*, *Neurog3*, *Neurod1*, *Isl1*, *Hnf6*, *Foxa2*, *Hnf1b* and *Sox9* in total pancreas of E13.5 $Glis3^{+/+}$ (white bars), $Glis3^{+/-}$ (grey bars) and $Glis3^{-/-}$ (black bars) mice as determined by quantitative RT-PCR (n=6). The housekeeping gene cyclophilin A was used as an internal control. Results are fold change relative to $Glis3^{+/+}$ mice, shown as the mean±SE; *p<0.05, **p<0.01 vs $Glis3^{+/+}$ mice. **b** *Neurog3* mRNA expression in the pancreas of $Glis3^{+/+}$ and $Glis3^{-/-}$ mice at E12.5, assayed by in situ hybridisation. **c** Immunostaining of PDX1 and NEUROG3 in the pancreas of $Glis3^{+/+}$ and $Glis3^{-/-}$ mice at E12.5. Nuclei were visualised by DAPI staining. Scale bar (**b, c**) 20 μm. **d** Quantification of NEUROG3-positive cells on E12.5 pancreatic immunostaining sections from $Glis3^{+/+}$ (n=5) and $Glis3^{-/-}$ (n=10) mice. **e** mRNA expression of *Glis3* and (**f**) *Neurog3* in PDCs transduced with pMSCV-*c-myc*-YFP or -*c-myc-Glis3* by quantitative RT-PCR (n=4). **p<0.01, ***p<0.001 vs YFP-treated cells

by the Notch gene homologue (NOTCH) [11, 35, 36] and TGFβ [37, 38] signalling pathways. To determine whether *Glis3* controls *Neurog3* expression indirectly through these modulators, we examined their expression in E13.5 pancreas by quantitative RT-PCR. We found that mRNA expression of *Pdx1, Hnf6, Sox9, Foxa2, Hnf1b, Notch1* to *Notch4, Hes1* and *Gdf11* occurred at similar levels in $Glis3^{-/-}$ to those in controls (Fig. 2a, ESM Fig. 4g).

As *Hes1* is a negative regulator of pancreatic endocrine cell fate determination [11, 36], we examined its expression in E12.5 embryos, a critical stage in endocrine cell fate determination. We found that hairy and enhancer of split 1 (*Drosophila*) (HES1) abundance was similar in E12.5 $Glis3^{-/-}$ and $Glis3^{+/+}$ pancreases (ESM Fig. 4e, f).

Taken together, these data indicate that *Glis3* inactivation leads to reduced *Neurog3* expression. However, downregula-

tion of *Neurog3* expression in *Glis3*$^{-/-}$ islets is not mediated indirectly by alterations in the expression of *Pdx1*, *Hnf6*, *Sox9*, *Foxa2*, *Hnf1b*, *Notch1* to *Notch4*, *Gdf11 or Hes1*.

GLIS3 binds to the Neurog3 promoter and activates Neurog3 gene transcription To investigate whether GLIS3 activates the *Neurog3* promoter directly, we cloned a 5.8 kb mouse *Neurog3* promoter-driven luciferase construct (*Neurog3*-Gluc). Luciferase assays revealed that *Glis3*, but not the *Glis3*-NDH1 mutant [7] significantly stimulated *Neurog3*-Gluc reporter activity in a beta cell (832/13 insulinoma cell) (Fig. 3a). To further localise the *cis*-element(s) in the *Neurog3* promoter through which GLIS3 regulates *Neurog3* transcription, we searched in the mouse *Neurog3* promoter for a GLIS3RE that we had recently uncovered in the insulin gene (GLIS3RE; 5′-GTCCCCTGCTGTGAA-3′) [7]. We identified five DNA elements that exhibited sequences very similar to GLIS3RE and were located at −4,692, −2,862, −2,718, −1,160 and −1,117 in this 5.8 kb promoter region (ESM Fig. 6).

To determine if GLIS3 does indeed bind to these five putative GLIS3REs in the endogenous *Neurog3* gene in cells, we first performed ChIP assays in PDCs transduced with *c-myc-Glis3*. The results showed that c-Myc-GLIS3 binds to all five putative GLIS3REs, but not to a control DNA sequence that is located in intron 1 (+7,963) of *Neurog3* (Fig. 3b). To further determine whether GLIS3 binds to any of these sites in vivo, we performed GLIS3 ChIP assays using wild-type fetal (E13.5) pancreases. We found that GLIS3 occupied all five putative GLIS3REs, being particularly enriched at the −2,718 and −1,117 sites, in the mouse *Neurog3* promoter of E13.5 fetal pancreas (Fig. 3c).

Next we performed EMSA using the DNA binding motif of GLIS3, the zinc finger domain. Of these five putative GLIS3REs, GLIS3 (zinc finger domain) was found to bind to the GLIS3RE probes at −2,862, −2,718, −1,160 and −1,117; the complexes were out-competed by molar excess of the corresponding non-biotinylated GLIS3REs. No binding was shown for the putative GLIS3RE at −4,692 (Fig. 3d).

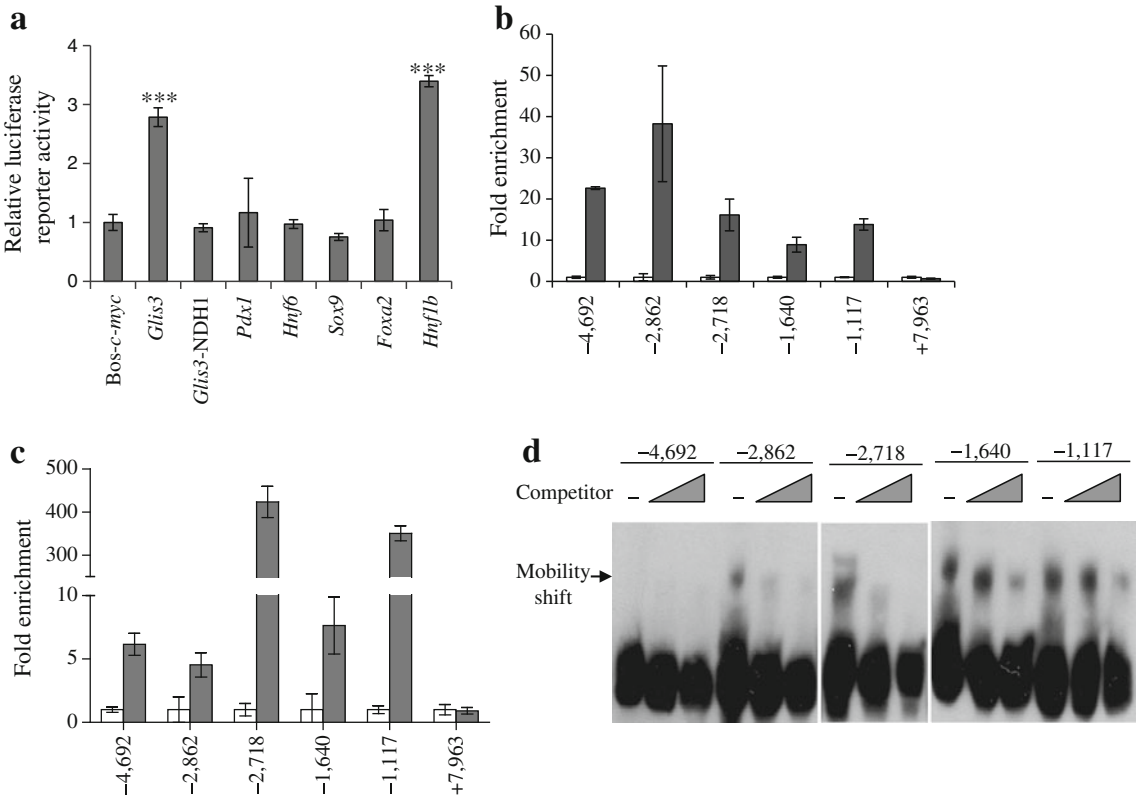

Fig. 3 GLIS3 activates *Neurog3* expression by directly binding to its promoter. **a** Promoter reporter assays performed in 832/13 cells co-transfected with the promoter reporter *Neurog3* (5.8 kb)-Gluc and Bos-*c-myc-Glis3*, or -*Glis3*-NDH1, -*Pdx1*, -*Hnf6*, -*Sox9*, -*Foxa2* or -*Hnf1b* (n=3). ***p<0.001 vs Bos-*c-myc* control. **b** ChIP was performed in PDCs transduced with pMSCV-*c-myc*-YFP (white bars) or -*c-myc-Glis3* (black bars), both with anti-c-Myc antibody, and (**c**) in pooled E13.5 pancreases with anti-GLIS3 antibody (black bars). White bars, IgG. Immunoprecipitated DNA was purified and analysed by quantitative PCR using primers specifically spanning putative GLIS3REs or a control fragment located in intron 1 (+7,963) in *Neurog3* promoter. **d** EMSA using an in vitro translated GLIS3-zinc finger domain peptide was performed with biotin-labelled probes containing putative GLIS3RE sequences as indicated. Five or twenty-five-fold unlabelled wild-type probes were added as competitors. Arrow, specific bands for mobility shift

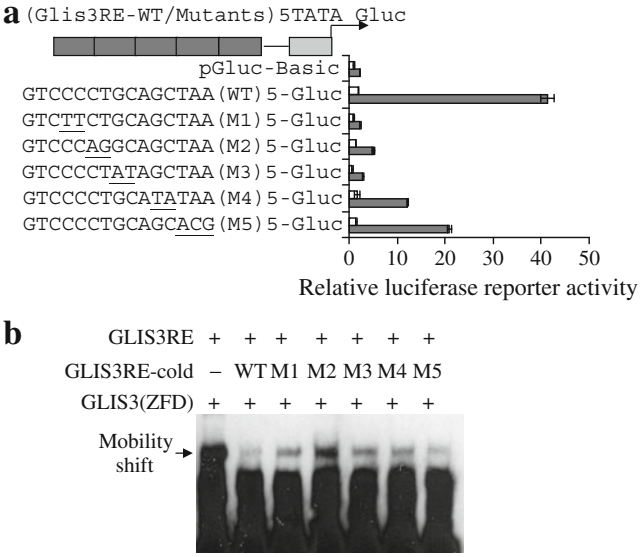

Fig. 4 GLIS3 binds to -2,718 GLIS3RE in mouse *Neurog3* promoter. **a** Schematic view of five tandem copies of the wild-type (WT) or mutated (M1–M5) GLIS3RE (−2,718) fused with *Neurog3* TATA box to drive expression of luciferase ([GLIS3RE]5-Gluc). Cells (832/13) were co-transfected with (GLIS3RE)5-Gluc and *c-myc-Glis3* (grey bars) or Bos-*c-myc* (white bars) constructs. The activity of each construct was normalised to that obtained with Bos-*c-myc*. **b** EMSA with an in vitro translated GLIS3-zinc finger domain (ZFD) peptide was performed using a biotin-labelled probe containing putative −2,718 GLIS3RE sequence as indicated (**a**). Tenfold non-labelled wild-type or mutated probes were added as competitors. Arrow, specific bands for mobility shift

Sequence alignment of homologous *Neurog3* promoter regions from mice, rats and humans showed that only one GLIS3RE, located between −2,718 and −2,703, was well conserved among the three species. We, therefore, generated five copies of the mouse −2,718 GLIS3RE and inserted it upstream of the pGluc-TATA box (−2,718 [GLIS3RE]5-Gluc). Five different mutant GLIS3REs were also generated to test GLIS3 binding specificity. We found that the −2,718 (GLIS3RE)5-Gluc construct was markedly activated by c-Myc-GLIS3. Each of the five serial mutants either abolished or profoundly attenuated the reporter activity (Fig. 4a). We used EMSA to further confirm the specificity of GLIS3RE binding (Fig. 4b). These results demonstrated that GLIS3 binds directly to several potential GLIS3REs in the mouse *Neurog3* promoter, particularly to the element at −2,718.

GLIS3 activates Neurog3 promoter synergistically with HNF6 and FOXA2 PDX1 [28–30], HNF6 [31], SOX9 [32], FOXA2 [33] and HNF1B [33, 34] have been reported to activate *Neurog3* gene promoter and stimulate *Neurog3* expression in fetal pancreas or in vitro. To determine the possible role of GLIS3 in the regulatory network of *Neurog3* transcription, we created constructs expressing *c-myc-Pdx1*, *-Hnf6*, *-Sox9*, *-Foxa2* and *-Hnf1b*, and co-transfected them with *Neurog3*-Gluc into HepG2 cells in the presence or absence of *c-myc-Glis3*. We found that *Neurog3*-Gluc activity was significantly stimulated by GLIS3, PDX1, HNF6, FOXA2 and HNF1B individually, but not by SOX9 (Fig. 5a). Furthermore, GLIS3 synergistically activated *Neurog3* reporter in combination with HNF6 or FOXA2, but not with PDX1, SOX9 or HNF1B (Fig. 5a). These results highlight an active role of GLIS3 in the transcriptional network of endocrine progenitors.

To establish whether GLIS3 physically interacts with HNF6 and FOXA2, we co-expressed *Glis3* with *c-myc-Hnf6* or *c-myc-Foxa2* in HepG2 cells and used an antibody against GLIS3 to immunoprecipitate GLIS3-interacting protein complexes from the nuclear extracts. Anti-c-Myc antibody detected c-Myc-HNF6 and -FOXA2, indicating that both transcription factors were co-precipitated with

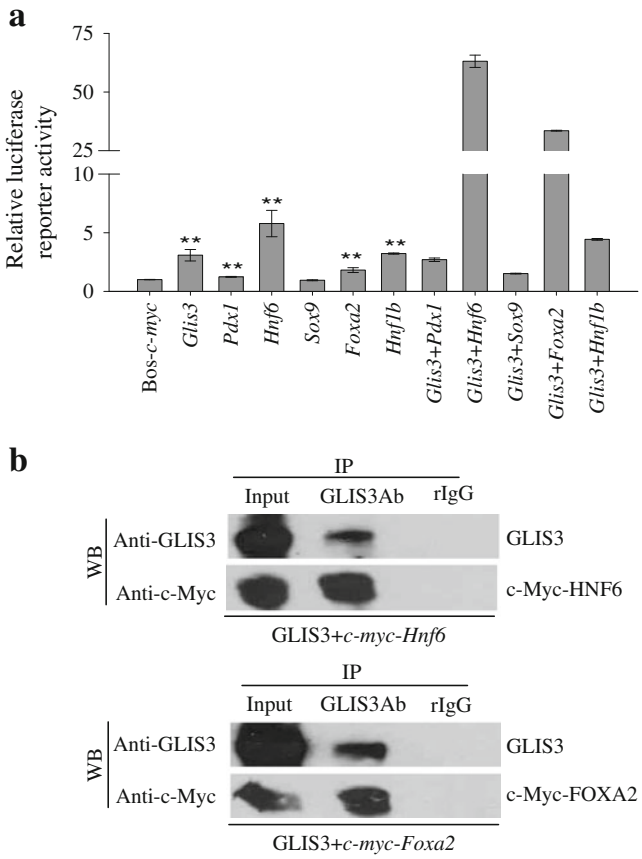

Fig. 5 GLIS3 transactivates *Neurog3* expression synergistically with HNF6 and FOXA2. **a** HepG2 cells co-transfected with *Neurog3* promoter reporter (−5.8 kb to 40 bp)-Gluc and individual *c-myc-Glis3*, *-Pdx1*, *-Hnf6*, *-Sox9*, *-Foxa2* and *-Hnf1b* or each in combination with *c-myc-Glis3*. Cells were co-transfected with CMV-β-galactosidase as a control. $^{**}p<0.01$ vs Bos-*c-myc* control. **b** HepG2 cells were co-transfected with *Glis3* and *c-myc-Hnf6* or *-Foxa2*. At 48 h after transfection, nuclear proteins were isolated and immunoprecipitated either with a rabbit anti-GLIS3 or rabbit IgG (rIgG) control. The immunoprecipitates were analysed with western blotting (WB) using anti-GLIS3 or anti-c-Myc antibody

GLIS3 (Fig. 5b), whereas pre-immune rabbit IgG failed to immunoprecipitate either complex. These results demonstrate that GLIS3 interacts with HNF6 and FOXA2 both physically and functionally to activate *Neurog3* gene transcription.

Discussion

In this study, we used in vivo and in vitro approaches to examine the function of GLIS3 in fetal mouse pancreas development. PDX1 is considered a master regulator of early pancreas specification [10, 21, 24] and NKX6-1 is a marker of early pancreatic epithelium specification [19, 20]. In *Glis3*-deficient mice, pancreatic levels of PDX1 and NKX6-1 were normal at E12.5, indicating that the pancreatic epithelium was normally specified in the absence of *Glis3*.

Once the pancreatic progenitor cells have been specified, the next important cell fate decision is whether the cells adopt an exocrine, ductal or endocrine fate. NEUROG3 promotes an islet fate within the domain of PDX1-positive cells [10–13]; therefore, in the absence of *Neurog3*, none of the major endocrine cell lineages can be formed [23]. Furthermore, ectopic expression of *Neurog3* in endodermal progenitor cells has been shown to program these cells into endocrine islet-like cells [39–41]. In contrast to the normal abundance of PDX1 and NKX6-1, NEUROG3 levels were significantly reduced in *Glis3*-deficient pancreases at E12.5, a finding that is consistent with the marked reduction of all five types of islet endocrine cells in the pancreas of $Glis3^{-/-}$ mice. Interestingly, from E15.5 onwards, all endocrine-related hormones and transcription factors examined by us were reduced in the islets of $Glis3^{-/-}$ embryos. Therefore, our studies suggest that the *Glis3* gene is functionally important in a critical time window in mouse endocrine pancreas development around E12.5 or E13.5, immediately before the secondary transition begins. This conclusion is supported by the significantly increased *Glis3* expression found at E12.5 in the fetal pancreas [9]. From E15.5 onwards, we found numerous defects in the islets of $Glis3^{-/-}$ mice, e.g. reduction of PDX1 and NKX6-1 abundance, which may be a secondary effect of the arrested normal islet development. *Neurog3* has been demonstrated to be a direct downstream target of *Pdx1* in fetal pancreas development [28]. Our study using $Glis3^{-/-}$ mice also places *Glis3* upstream of *Neurog3* during early pancreas development.

We examined whether *Neurog3* is a direct downstream target of *Glis3* in experiments involving beta and non-beta cell lines. We found that c-Myc-GLIS3 was sufficient to stimulate endogenous *Neurog3* mRNA expression in PDCs, suggesting that *Neurog3* is a downstream target of *Glis3*. Next, using a combination of luciferase reporter analyses, ChIP assays (in PDCs and in E13.5 pancreases) and EMSA, we identified four GLIS3-binding sites in the mouse *Neurog3* promoter region. The discrepancy between ChIP and EMSA for the −4692 site may have been caused by the different sensitivities of the ChIP and EMSA assays, or by the presence of a site that was covered by the primers used in the ChIP (covering 140 bp), but not by the EMSA assay with its smaller span (covering only 30 bp). It is noteworthy that the fetal pancreases analysed by ChIP showed the best conserved GLIS3RE among different species at −2718 to be the strongest among all elements tested. These data support the conclusion that *Neurog3* is a direct downstream target of *Glis3* in the transcriptional hierarchy of pancreas development.

Neurog3 gene expression is tightly regulated by a network of positive regulators such as PDX1 [28–30], HNF6 [31], SOX9 [32], FOXA2 [33] and HNF1B [33, 34], as well as by negative regulators such as those in the Notch [11, 35, 36] and TGFβ [37, 38] signalling pathways. However, *Glis3* does not seem to control *Neurog3* expression through these positive and negative modulators of *Neurog3* expression, because quantitative PCR showed similar expression levels of all these modulators in $Glis3^{-/-}$ and $Glis3^{+/+}$ embryos.

In addition to directly controlling *Neurog3* transcription, GLIS3 was shown here to physically interact with HNF6 and FOXA2 in co-precipitation experiments; it also synergistically activated *Neurog3* promoter when co-expressed with each of the above transcription factors. Therefore, in addition to direct activation of *Neurog3* transcription via GLIS3RE in the *Neurog3* promoter, GLIS3 also functions in a combinatorial manner with other transcription factors, underscoring the multiple functions of GLIS3 within the regulatory network of *Neurog3* gene expression.

In conclusion, we used genetic mouse models and in vitro experiments to define the molecular interactions and functions of GLIS3 in regulating the differentiation of pancreatic endocrine progenitors. We found that GLIS3 binds to the *Neurog3* promoter and directly activates *Neurog3* gene transcription; it also activates *Neurog3* expression synergistically with two other *Neurog3*-activators, HNF6 and FOXA2. Therefore, loss of *Glis3* function produces defective *Neurog3* activation, which results in impaired fetal islet differentiation and neonatal diabetes.

Acknowledgements We thank AK Rustgi (University of Pennsylvania, School of Medicine, Philadelphia, PA, USA) for PDCs, C. Newgard (Duke University, Durham, NC, USA) for 832/13 cells, C. Wright (Vanderbilt University, Nashville, TN, USA) for goat anti-PDX1 antibody; Developmental Studies Hybridoma Bank (University of Iowa, Iowa City, IA, USA) for anti-NEUROG3 and anti-NKX6-1 antibodies; W. Qian, A. Liang and Integrated Microscopy Core (Baylor College of Medicine) for technical support. This research was supported by the US National Institutes of Health (NIH) grant DK-68037 (to L. Chan), the Diabetes and Endocrinology Research Center (P30DK079638), the Betty Rutherford Chair from St Luke's Episcopal Hospital and the T.T. & W.F. Chao Foundation.

Contribution statement YY, BH-JC and LC designed the study, analysed and interpreted the data, drafted and revised the manuscript. VY, WC and MJT participated in the study design, analysed and interpreted the data, and revised the manuscript. LL participated in the study design, analysed the data, and revised the manuscript. All authors have approved the final version of the manuscript.

Duality of interest The authors declare that there is no duality of interest associated with this manuscript.

References

1. Hamilton-Shield JP (2007) Overview of neonatal diabetes. Endocr Dev 12:12–23
2. Barbetti F (2007) Diagnosis of neonatal and infancy-onset diabetes. Endocr Dev 11:83–93
3. Greeley SA, Tucker SE, Naylor RN, Bell GI, Philipson LH (2010) Neonatal diabetes mellitus: a model for personalized medicine. Trends Endocrinol Metab 21:464–472
4. Taha D, Barbar M, Kanaan H, Williamson BJ (2003) Neonatal diabetes mellitus, congenital hypothyroidism, hepatic fibrosis, polycystic kidneys, and congenital glaucoma: a new autosomal recessive syndrome? Am J Med Genet A 122A:269–273
5. Kim YS, Nakanishi G, Lewandoski M, Jetten AM (2003) GLIS3, a novel member of the GLIS subfamily of Kruppel-like zinc finger proteins with repressor and activation functions. Nucleic Acids Res 31:5513–5525
6. Senee V, Chelala C, Duchatelet S, Feng D, Blanc H, Cossec JC et al (2006) Mutations in GLIS3 are responsible for a rare syndrome with neonatal diabetes mellitus and congenital hypothyroidism. Nat Genet 38:682–687
7. Yang Y, Chang BH, Samson SL, Li MV, Chan L (2009) The Kruppel-like zinc finger protein Glis3 directly and indirectly activates insulin gene transcription. Nucleic Acids Res 37:2529–2538
8. Watanabe N, Hiramatsu K, Miyamoto R et al (2009) A murine model of neonatal diabetes mellitus in Glis3-deficient mice. FEBS Lett 583:2108–2113
9. Kang HS, Kim YS, ZeRuth G et al (2009) Transcription factor Glis3, a novel critical player in the regulation of pancreatic beta-cell development and insulin gene expression. Mol Cell Biol 29:6366–6379
10. Gu G, Dubauskaite J, Melton DA (2002) Direct evidence for the pancreatic lineage: NGN3+ cells are islet progenitors and are distinct from duct progenitors. Development 129:2447–2457
11. Apelqvist A, Li H, Sommer L et al (1999) Notch signalling controls pancreatic cell differentiation. Nature 400:877–881
12. Schwitzgebel VM, Scheel DW, Conners JR et al (2000) Expression of neurogenin3 reveals an islet cell precursor population in the pancreas. Development 127:3533–3542
13. Jensen J, Heller RS, Funder-Nielsen T et al (2000) Independent development of pancreatic alpha- and beta-cells from neurogenin3-expressing precursors: a role for the notch pathway in repression of premature differentiation. Diabetes 49:163–176
14. Lee EC, Yu D, Martinez DV et al (2001) A highly efficient Escherichia coli-based chromosome engineering system adapted for recombinogenic targeting and subcloning of BAC DNA. Genomics 73:56–65
15. Nagy A, Rossant J, Nagy R, Bramow-Newerly W, Roder JC (1993) Derivation of completely cell culture-derived mice from early-passage embryonic stem cells. Proc Natl Acad Sci USA 90:8424–8428
16. O'Gorman S, Dagenais NA, Qian M, Marchuk Y (1997) Protamine-Cre recombinase transgenes efficiently recombine target sequences in the male germ line of mice, but not in embryonic stem cells. Proc Natl Acad Sci USA 94:14602–14607
17. Schreiber FS, Deramaudt TB, Brunner TB et al (2004) Successful growth and characterization of mouse pancreatic ductal cells: functional properties of the Ki-RAS(G12V) oncogene. Gastroenterology 127:250–260
18. Mizushima S, Nagata S (1990) pEF-BOS, a powerful mammalian expression vector. Nucleic Acids Res 18:5322
19. Sander M, Sussel L, Conners J et al (2000) Homeobox gene Nkx6.1 lies downstream of Nkx2.2 in the major pathway of beta-cell formation in the pancreas. Development 127:5533–5540
20. Nelson SB, Schaffer AE, Sander M (2007) The transcription factors Nkx6.1 and Nkx6.2 possess equivalent activities in promoting beta-cell fate specification in Pdx1+ pancreatic progenitor cells. Development 134:2491–2500
21. Oliver-Krasinski JM, Stoffers DA (2008) On the origin of the beta cell. Genes Dev 22:1998–2021
22. Jorgensen MC, Ahnfelt-Ronne J, Hald J, Madsen OD, Serup P, Hecksher-Sorensen J (2007) An illustrated review of early pancreas development in the mouse. Endocr Rev 28:685–705
23. Gradwohl G, Dierich A, LeMeur M, Guillemot F (2000) Neurogenin3 is required for the development of the four endocrine cell lineages of the pancreas. Proc Natl Acad Sci USA 97:1607–1611
24. Murtaugh LC (2007) Pancreas and beta-cell development: from the actual to the possible. Development 134:427–438
25. Huang HP, Liu M, El-Hodiri HM, Chu K, Jamrich M, Tsai MJ (2000) Regulation of the pancreatic islet-specific gene BETA2 (neuroD) by neurogenin 3. Mol Cell Biol 20:3292–3307
26. Gasa R, Mrejen C, Leachman N et al (2004) Proendocrine genes coordinate the pancreatic islet differentiation program in vitro. Proc Natl Acad Sci USA 101:13245–13250
27. Heremans Y, van de Casteele M, In't Veld P et al (2002) Recapitulation of embryonic neuroendocrine differentiation in adult human pancreatic duct cells expressing neurogenin 3. J Cell Biol 159:303–312
28. Oliver-Krasinski JM, Kasner MT, Yang J et al (2009) The diabetes gene Pdx1 regulates the transcriptional network of pancreatic endocrine progenitor cells in mice. J Clin Invest 119:1888–1898
29. Jiang J, Au M, Lu K et al (2007) Generation of insulin-producing islet-like clusters from human embryonic stem cells. Stem Cells 25:1940–1953
30. Miyazaki S, Yamato E, Miyazaki J (2004) Regulated expression of pdx-1 promotes in vitro differentiation of insulin-producing cells from embryonic stem cells. Diabetes 53:1030–1037
31. Jacquemin P, Durviaux SM, Jensen J et al (2000) Transcription factor hepatocyte nuclear factor 6 regulates pancreatic endocrine cell differentiation and controls expression of the proendocrine gene ngn3. Mol Cell Biol 20:4445–4454
32. Lynn FC, Smith SB, Wilson ME, Yang KY, Nekrep N, German MS (2007) Sox9 coordinates a transcriptional network in pancreatic progenitor cells. Proc Natl Acad Sci USA 104:10500–10505
33. Lee JC, Smith SB, Watada H et al (2001) Regulation of the pancreatic pro-endocrine gene neurogenin3. Diabetes 50:928–936
34. Maestro MA, Boj SF, Luco RF et al (2003) Hnf6 and Tcf2 (MODY5) are linked in a gene network operating in a precursor cell domain of the embryonic pancreas. Hum Mol Genet 12:3307–3314
35. Hald J, Hjorth JP, German MS, Madsen OD, Serup P, Jensen J (2003) Activated Notch1 prevents differentiation of pancreatic acinar cells and attenuate endocrine development. Dev Biol 260:426–437
36. Murtaugh LC, Stanger BZ, Kwan KM, Melton DA (2003) Notch signaling controls multiple steps of pancreatic differentiation. Proc Natl Acad Sci USA 100:14920–14925

37. Dichmann DS, Yassin H, Serup P (2006) Analysis of pancreatic endocrine development in GDF11-deficient mice. Dev Dyn 235:3016–3025
38. Harmon EB, Apelqvist AA, Smart NG, Gu X, Osborne DH, Kim SK (2004) GDF11 modulates NGN3+ islet progenitor cell number and promotes beta-cell differentiation in pancreas development. Development 131:6163–6174
39. Grapin-Botton A, Majithia AR, Melton DA (2001) Key events of pancreas formation are triggered in gut endoderm by ectopic expression of pancreatic regulatory genes. Genes Dev 15:444–454
40. Johansson KA, Dursun U, Jordan N et al (2007) Temporal control of neurogenin3 activity in pancreas progenitors reveals competence windows for the generation of different endocrine cell types. Dev Cell 12:457–465
41. Yechoor V, Liu V, Espiritu C et al (2009) Neurogenin3 is sufficient for transdetermination of hepatic progenitor cells into neo-islets in vivo but not transdifferentiation of hepatocytes. Dev Cell 16:358–373